Extended Abstracts of the 2013 International Conference on Solid State Devices and Materials, Fukuoka, 2013, pp296-297

Ballistic Transport of Massless Dirac Fermions in Graphene

Yohta Sata[1], Satoru Masubuchi[1,2], Masahiro Onuki[1], Takehiro Yamaguchi[1]
Kenji Watanabe[3], Takashi Taniguchi[3], and Tomoki Machida[1,2,4]

[1] Institute of Industrial Science, University of Tokyo
4-6-1 Komaba Meguro-ku, Tokyo 153-8505, Japan
Phone: +81-3-5452-6158 E-mail: ysata@iis.u-tokyo.ac.jp
[2] Institute for Nano Quantum Information Electronics, University of Tokyo,
4-6-1 Komaba Meguro-ku, Tokyo 153-8505, Japan
[3] National Institute for Material Science,
1-1 Namiki, Tsukuba 305-0044, Japan
[4] PRESTO-JST,
4-1-8 Honcho, Kawaguchi, Saitama 332-0012, Japan

Abstract

We report on the nonlocal magnetotransport measurements in ballistic graphene Hall-bar devices fabricated on hexagonal boron nitride. The value of nonlocal resistance R_{NL} shows peak structures at magnetic fields, where the cyclotron diameter $2R_c$ equals integer multiple of the separation length between voltage probes L, indicating the observation of transverse magnetic focusing effect of ballistic charge carriers travelling from source to voltage probes. The emergence of ballistic transport in graphene/h-BN allowed us to develop current rectification devices, which utilize the charge carrier reflection at sample boundaries for guiding electrons to predestined direction.

1. Introduction

Owing to a linear energy dispersion relation, charge carriers in graphene behave as massless Dirac fermions [1, 2]. Since the charge carrier motion in graphene is governed by relativistic quantum physics, graphene exhibits novel transport phenomena such as Klein-tunneling and evanescent-wave transport. For the understandings of transport properties of graphene, investigations for charge carrier transport phenomena where the charge carriers travel without scattering for macroscopic distances *i.e.* ballistic regime is highly desired. In addition, ballistic transport phenomena in semiconductor system are of high importance for developing electronic devices such as three-terminal ballistic junctions [3] and ballistic rectifiers [4].

Recent developments in mechanical transfer technique of graphene on hexagonal boron nitride have enabled high-quality substrate-supported graphene, which exhibits charge carrier mobility of $\mu \sim 100{,}000$ cm^{2}V^{-1}s^{-1}. In such high-mobility graphene, the mean free path of charge carriers reaches on the order of microns at room temperature, which is comparable to the sample size, and charge carriers travel ballistically. Therefore, graphene on hexagonal boron nitride can be utilized as a platform for studying the ballistic transport phenomena of massless Dirac fermions in graphene, and can be a unique platform for developing ballistic electronic devices that operate at room temperature.

2. Coherent Electron Focusing Effect

The graphene/hexagonal boron nitride heterostructure was fabricated using the mechanical transfer technique of monolayer graphene [5]. First, we deposited a 50 nm thick h-BN flake by mechanical exfoliation of h-BN on a Si wafer with a thermally oxidized layer of 290 nm thick SiO_2. Monolayer graphene flake was then deposited on a separate Si wafer with a spin-coated polymethylmethacrylate (PMMA) layer. The graphene on PMMA layer was transferred onto the h-BN crystal using an alignment technique under an optical microscope. Then, Hall-bar geometry was defined using the standard electron-beam lithography and subsequent oxygen plasma etching technique [Fig. 1]. Metal contacts were fabricated by electron beam lithography followed by the evaporation of Pd (80 nm) and lift-off. The resist residues were removed by annealing in Ar/H_2

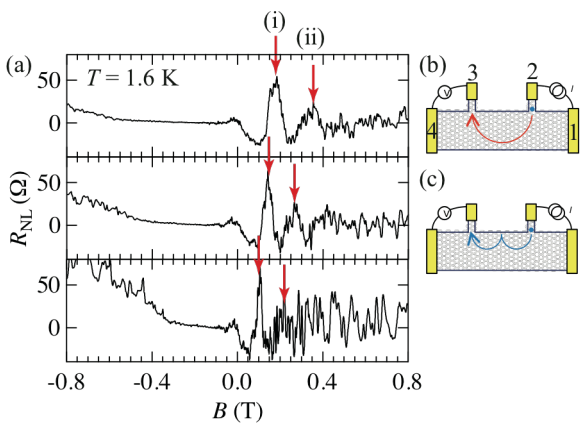

Fig. 1 (a) Nonlocal resistance R_{NL} as a function of magnetic field B for varying back-gate bias voltage V_{BG} = 30, 20, and 10 V (top to bottom) measured at T = 1.6 K. (b) The schematics of electron trajectory in Hall-bar device in condition that cyclotron diameter equals $R_c = L$ (i) and $2L$ (ii).

(97:3) gas flow for 5 h.

The measurements were performed in a ^{4}He-cooled variable temperature insert at temperature of T = 1.5 K. Transport measurements were carried out using the standard lock-in technique. Nonlocal resistance $R_{NL} = V/I_{ac}$ was measured by applying a small alternating current of I_{ac} = 100 nA between terminal 1 and 2, and measuring voltage V between terminals 3 and 4 [Fig. 1(b)]. Magnetic fields were applied perpendicularly to the sample surface using the superconducting magnet. A conducting Si substrate was used as a global back gate to tune charge carrier density as $n = C_g(V_g - D_{irac})$ where $C_g = 1.07\text{x}10^{-4}$ F/m^2 is the gate-capacitance and D_{irac} is the value of V_g at charge neutrality point.

Fig. 1 (a) shows nonlocal resistance R_{NL} as a function of magnetic field B measured at back-gate bias voltages V_{BG} = 30, 20, and 10 V (top to bottom). First, we focus on the data for V_{BG} = 30 V. When the magnetic field was increased from zero, the value of R_{NL} oscillated as a function of B, whose peak structures were located at B = 0.4, 0.8, and 1.2 T (black arrows in Fig. 1(a)). On the other hand, when the magnetic field was decreased from zero, the value of R_{NL} showed no oscillation behavior. When the back-gate bias voltage was decreased as V_{BG} = 20 and 10 V, the positions of peak structures for $B > 0$ were shifted to the smaller values of B.

The peak positions were shown to be located at magnetic fields, where the cyclotron diameter $2R_c$ equals integer multiple of the separation length between voltage probes L, since the cyclotron radius can be written as a function of charge carrier density $R_c = (\hbar/eB)\sqrt{\pi n}$. This observation indicates that the peak structures in R_{NL} were induced by the charge carriers travelling from source to voltage probes ballistically as schematically depicted in Figs. 1(b) and (c), where the first peak corresponds to electrons travelling directly from the source to the voltage probe [Fig. 1(b)], and the second peak corresponds to electrons reflected off the edge before reaching the voltage probe [Fig. 1(c)]. This observation demonstrates that the charge carriers in our device travels ballistically in the channel and are focused onto the voltage probe by the cyclotron motion, indicating the observation of the magnetic focusing effect in our graphene device.

3. Current Rectification in Ballistic Antidot System

The emergence of ballistic transport in graphene/h-BN allowed us to current rectification devices, which utilize the ballistic transport of charge carriers in graphene, whose device structure is shown in Fig. 2. The central region of the device was etched away by oxygen plasma forming antidot system. This region guides ballistic electrons injected from right (R) and left (L) contacts toward the bottom voltage contact (V^-) as schematically indicated in Fig. 2. As a result, the electrons are focused to the predetermined direction independent of current direction, which induces voltage signals in the lower voltage contact. The device operates similar to a bridge rectifier [Fig. 2(b)], however

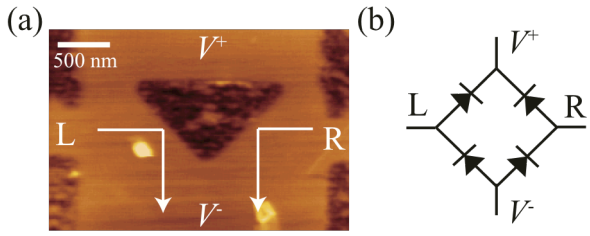

Fig. 2 Atomic Force Microscopy Image of the device studied in this work. The characters R, L, and D indicate Right, Left and Drain probes respectively.

since the operation principle is completely different, and suitable for operation in high frequencies. We will discuss the characterization of current rectification devices as a function of operation temperature and frequencies.

4. Conclusion

In this work, we conducted magnetotransport measurements in ballistic graphene Hall-bar devices deposited on hexagonal boron nitride. Our graphene devices exhibited distinct oscillation in nonlocal resistance R_{NL}, which was attributed to magnetic focusing effect of charge carriers in graphene, indicating that ballistic charge carrier transport devices can be developed using graphene. This observation lead to fabricating current rectification devices using graphene, suggesting that it could be possible route for developing flexible and transparent electronic devices using graphene.

Acknowledgements

The authors acknowledge R. Moriya for technical support and helpful discussions. This study was supported by the PRESTO, Japan Science and Technology agency, the Grants-in-Aid from the MEXT, the CREST Japan Science and technology Agency, and the Project for Developing Innovation Systems of the MEXT.

References

[1] K. S. Novoselov, A. K. Geim, S. V. Morozov, D. Jiang, M. I. Katsnelson, I. V. Grigorieva, S. V. Dubonos, and A. A. Firsov, Nature 438, 197 (2005).

[2] Y. Zhang, Y. W. Tan, H. L. Stormer, and P. Kim, Nature **438**, 201 (2005).

[3] I. Shorubalko, H. Q. Xu, P. Omling, and L. Samuelson Appl. Phys. Lett. **83**, 2369 (2003).

[4] A. M. Song, A. Lorke, A. Kriele, and J. P. Kotthaus, Phys. Rev. Lett. **80**, 3831 (1998).

[5] C. R. Dean, A. F. Young, *et al.*, Nature Nanotechnology **22**, 722 (2010).

[6] H. van Houten *et al.*, Phys. Rev. B **39**, 8556 (1989).